

A Uniform Optimum Material Based Model for Concurrent Optimization of Thermoelastic Structures and Materials

Jun Yan^{1a}, Geng-dong Cheng¹, Ling Liu¹

¹ State Key Lab of Structural Analysis for Industrial Equipment and Department of Engineering Mechanics, Dalian University of Technology, Dalian, 116024, P.R.China

Received 08 May 2008, Accepted 03 September 2008

Abstract –This paper presents an optimization technique for structures composed of uniform cellular materials in macro scale. The optimization aims at to obtain optimal configurations of macro scale structures and microstructures of material under certain mechanical and thermal loads with specific base material volume. A concurrent topology optimization method is proposed for structures and materials to minimize compliance of thermoelastic structures. In this method macro and micro densities are introduced as the design variables for structure and material microstructure independently. Penalization approaches are adopted at both scales to ensure clear topologies, i.e. SIMP (Solid Isotropic Material Penalization) in micro-scale and PAMP (Porous Anisotropic Material Penalization) in macro-scale. Optimizations in two scales are integrated into one system with homogenization theory and the distribution of base material between two scales can be decided automatically by the optimization model. Microstructure of materials is assumed to be uniform at macro scale to reduce manufacturing cost. The proposed method and computational model are validated by the numerical experiments. The effects of temperature differential, volume of base material, numerical parameters on the optimum results are also discussed. At last, for cases in which both mechanical and thermal loads apply, the configuration of porous material can help to reduce the system compliance.

Key words: Topology optimization, thermoelasticity, concurrent optimization, porous anisotropic material, homogenization

1 Introduction

With shortage of global resources and the intense of enterprises' competition, structural optimization design is drawing more and more attention from academicians and engineers. Different from dimensional or shape optimization, structural topology optimization can achieve more efficient conception/configuration design at the stage of initial design, and it is a hot topic in recent two decades. The pioneer work of structural topology optimization for continuum can be traced back to 1981, when Cheng and Olhoff[1] introduced the concept of microstructure to structural optimization in their studies of optimum thickness design of a solid elastic plate with minimum compliance. After that, Homogenization method[2] and SIMP(Solid Isotropic Material with Penalization) method[3] were developed and became two main branches of topology optimization.

Structures could be frequently applied with mechanical and thermal loads simultaneously in automobile, electronic, nuclear, aerospace and aircraft industries. It is worth of mentioning that some new materials that sustain extreme temperature are often bear mechanical loads also in practical structures. Thus studies of optimization design of this kind of thermoelastic structures are becoming a very attractive area. But there are no enough papers to deal with the topology optimization for structures and materials with combined mechanical and thermal loads, especially for the concurrent optimization for the two scales simultaneously to consider the coupled effects of macro-structure and micro-structure. [4; 5].

This paper presents an optimization technique for thermoelastic structures composed of uniform cellular materials in macro scale. The optimization aims at to obtain optimal configurations of macro scale structures and microstructures of material under certain mechanical and thermal loads with specific base material volume. A concurrent topology optimization method is proposed for structures and materials to minimize compliance of structures. In this method macro and micro densities are introduced as the design variables for structure and material microstructure independently. Penalization approaches are adopted at both scales to ensure clear topologies, i.e. SIMP (Solid Isotropic Material Penalization) in micro-scale and PAMP (Porous Anisotropic Material Penalization) in macro-scale. Optimizations in two scales are integrated into one system with homogenization theory and the distribution of base material between two scales can be decided automatically by the optimization model. Microstructure of materials is assumed to be uniform at macro scale to reduce manufacturing cost. The proposed method and computational model are validated by the numerical experiments. The effects of temperature differential, volume of base material, numerical parameters on the optimum results are also discussed. At last, for cases in which both mechanical and thermal loads apply, the configuration of porous material can help to reduce the system compliance.

2 Concurrent optimization of structures and materials

Microstructure with some simple specific configurations is introduced into topology optimizations in homogenization

^a Corresponding author: yanjun@dlut.edu.cn

method and is assumed with infinite periods normally. Then structural topology optimization can be solved by size optimization in micro scale. The “Black-White” design of macro structures can be realized according to the relative density of unit cells of materials. Cells with large cavities (representing

“white”) are treated as void, while those with small cavities (representing “black”) denote solid part and form the structure. Though unit cells are introduced into homogenization method, the optimization at micro scale is limited to be within the scope of size optimization.

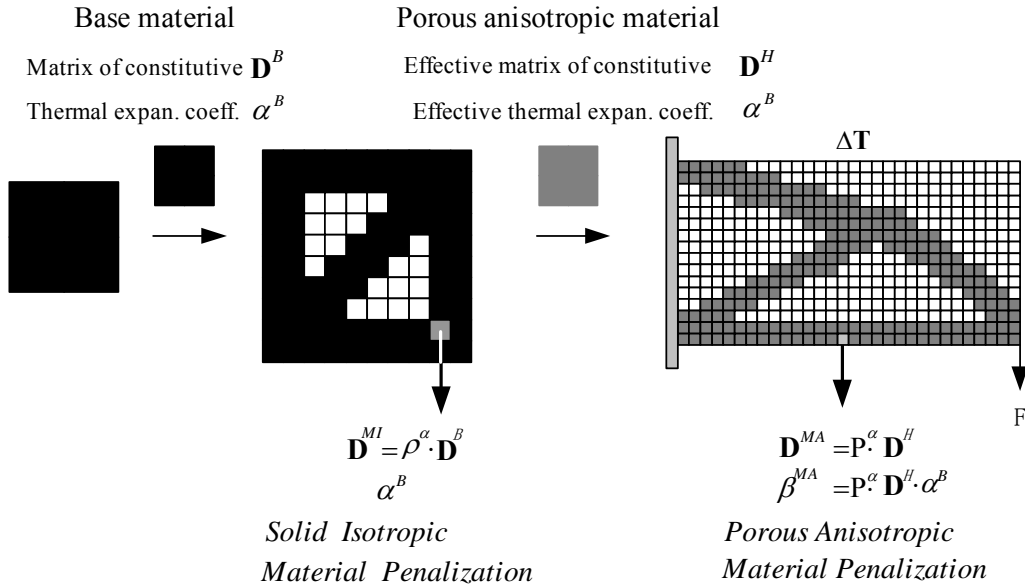


Fig. 1. Penalization-based concurrent optimization with two classes of density as design variables

An alternative approach to implement structural topology optimization is the so-called SIMP method. Densities of elements are set as design variables to interpolate the transition between solid material and void. Relationship between the design variable and the material properties is established based on power laws, which are mental assumptions. Though having been proposed to match with the intermediate densities in the sense of effective elastic properties[6], microstructures are introduced merely for validating the material interpolation model but not integrated into the optimization.

Application of the above two approaches often leads to structural design containing gray area, which is neither solid nor void, and checkerboard pattern. To achieve clear “black-white” topology, various techniques [3] have been developed, such as enforcing an upper bound on the perimeter of structures [7], introducing a filtering function[8] and imposing constraints on the slope of the parameters defining the geometry[9].

Rodrigues et al.[10] proposed a hierarchical design method for structure and material to achieve minimum system compliance with a homogenization method. This method is characterized by the varying microstructural configurations from point to point in macro-scale, which results in a “varying gray” look of the structural design. Such results could bring about some manufacturing difficulty. It must be pointed out that the design variables for macro and micro scales in this method are dependent, that is to say, the ratio of integration of micro-density (micro design variables) over micro unit cell to the volume of micro unit cell is set to be equal to the macro-density(macro design variables).

The ultra-light material includes metal cellular materials with perfect periodic micro-structural arrangement, such as metal honeycomb materials, metal linear cellular alloys and truss-like materials. With rapid developments in manufactur-

ing techniques, ultra-light material are increasingly widely used in applications such as ultra-light weight structures, heat exchangers, energy absorption systems, vibration control and acoustical scattering[11; 12; 13]. But a new problem rises in field of topology optimization with the increasing use of ultra-light materials in which macro relative density is no longer 1 but an intermediate value between 0 and 1. That is how to design an optimal structure and corresponding material microstructure with homogeneous cellular material in macro scale. And we note that many research works[14; 15; 16; 17] for ultra-light materials aim only at developing materials with prescribed or extreme properties, i.e., optimizing material microstructure in terms of certain equivalent properties(pure tension, bending or torsion) which is not guaranteed to be the most efficient when constructing the structure, since both structural configuration and boundary condition may vary dramatically in practical use.

The present work attempts to achieve a “single gray-white” design as shown in Fig 1. In macro scale, the “gray domain” is occupied by macro homogeneous porous material; the “white domain” has no material distribution. In micro scale, for porous material in “gray domain”, the “black domain” in microstructure is occupied by base material such as aluminum or its alloy; and the “white domain” has no material. Especially the porous materials are usually anisotropic and its microstructures are free from any assumptions about its configurations (e.g. cellular materials with square and rectangular holes, ranked laminates). To obtain such a design, we will establish the mathematics formulae for concurrent optimization in next section.

3 Formulation of optimization

Both problems at macro-structure and micro-structure scales as shown in Fig 1 can be dealt with as classical layout de-

signs, for which topology optimization is a powerful tool. First as shown in Figure 1, macro domain Ω is meshed into N elements and micro domain Y is meshed into n elements. Each element is then assigned a unique density value varying between 0 and 1, e.g. P_i for the i th ($i=1,2,\dots,N$) element in macro-scale and ρ_j ($j=1,2,\dots,n$) for the j th element in micro-scale. Since elements in macro-scale is composed of porous material, its physical density equals to $\rho^{PAM} \times P_i(X)$, where $\rho^{PAM} = \int_Y \rho dy / V^{MI}$, relative density of the porous anisotropic material, is included here. In single-scaled topology optimization, the relative density ρ^{PAM} should equal to 1. Y represents micro design domain and V^{MI} is the area of micro design domain. The macro design domain Ω is subjected to external forces \mathbf{F} and uniform temperature differential ΔT , then the formulation of optimization for the minimum compliance can be expressed as

$$\text{Min} : C = \int_{\Omega} \mathbf{F} \cdot \mathbf{U} d\Omega + \int_{\Omega} \boldsymbol{\beta}^{MA} \cdot \boldsymbol{\varepsilon} \cdot \Delta T d\Omega \quad (1)$$

$$\text{s.t.} : \mathbf{K} \left(P^\alpha E^H(\rho) \right) \cdot \mathbf{U} = \mathbf{F}^{Me} + \mathbf{F}^{TEM} \left(P^\alpha \boldsymbol{\beta}^H(\rho) \right) \quad (2)$$

$$\text{s.t.} : \zeta = \frac{\rho^{PAM} \cdot \int_{\Omega} P d\Omega}{V^{MA}} \leq \bar{\zeta} \quad (3)$$

$$\text{s.t.} : \gamma = \sum_{k=1}^m l_k \cdot (\rho_{k1} - \rho_{k2})^2 \leq \bar{\gamma} \quad (4)$$

$$\text{s.t.} : 0 < \delta \leq P \leq 1, 0 < \delta \leq \rho \leq 1 \quad (5)$$

where C denotes structural compliance and \mathbf{U} , $\boldsymbol{\varepsilon}$ represent structural deformation vector and strain tensor, $\boldsymbol{\beta}^{MA}$ represents the effective thermal stress tensor of porous material in macro scale.

Constraint I represents the balance equation for macro-structure system which shows how the two independent design variables (P, ρ) influence the stiffness matrix \mathbf{K} and thermo-load vector \mathbf{F}^{TEM} . More detailed explanations about this constraint can be found at section 4.

Constraint II sets a limit on the total available base material by defining relative density ζ and its upper bound $\bar{\zeta}$. V^{MA} is the area of macro design domain Ω .

To limit the complexity of designs and suppress the checkerboard pattern, Constraint III, a so called ‘‘perimeter-like’’ constraint[18] is introduced in this research where m is the number of share edge in finite element mesh, l_k is the length of share edge, ρ_{k1}, ρ_{k2} are the micro densities of neighbor elements who share the k th edge, and $\bar{\gamma}$ is specific upper bounds of perimeter.

Constraint IV sets bounds for density variables at two scales to avoid numerical singularity of optimization, where

δ is a small predetermined value that is set as $\delta = 0.001$ here.

4 Structure and sensitivity analysis for thermoelastic structures

4.1 Structural analysis for thermoelastic structures

The compliance of thermoelastic structures show in Eq. [1] can be obtained by Finite element analysis. The formula are shown as follows,

$$\mathbf{K} \cdot \mathbf{U} = \mathbf{F}^{Me} + \mathbf{F}^{TEM} \quad (6)$$

$$\mathbf{K} = \int_{\Omega} \mathbf{B}^T \mathbf{D}^{MA} \mathbf{B} d\Omega \quad (7)$$

$$\mathbf{F}^{TEM} = \int_{\Omega} \mathbf{B} \cdot \boldsymbol{\beta}^{MA} \cdot \Delta T d\Omega \quad (8)$$

Here, \mathbf{K} is stiffness matrix of structures and \mathbf{B} is the strain-displacement matrix. \mathbf{U} and ΔT are the vectors composed of the nodal values of \mathbf{U} and ΔT . \mathbf{F}^{Me} and \mathbf{F}^{TEM} represent the vectors of mechanical loads and thermal loads respectively. \mathbf{D}^{MA} and $\boldsymbol{\beta}^{MA}$ are the elastic constitutive matrix and the thermal stress matrix of macro material points to be determined by the following equations.

$$\mathbf{D}^{MA} = P^\alpha \cdot \mathbf{D}^H \quad (9)$$

$$\boldsymbol{\beta}^{MA} = P^\alpha \cdot \mathbf{D}^H \cdot \boldsymbol{\alpha}^H \quad (10)$$

P is the design variable defined as the macro density, α denotes the exponent of penalization and $\alpha = 3$ here. $\boldsymbol{\alpha}^H$ represents effective thermal expansion coefficients matrix. According to reference [19], no matter what configuration of micro unit cell has, we always have $\boldsymbol{\alpha}^H = \boldsymbol{\alpha}^B$ for porous anisotropic material composed of one pure base material, $\boldsymbol{\alpha}^B$ being thermal expansion coefficients matrix of base material. \mathbf{D}^H is the equivalent macro elastic constitutive matrix with corresponding macro relative density being 1. The computation of \mathbf{D}^H could follow the classical homogenization procedures[2] :

$$\mathbf{D}^H = \frac{1}{|Y|} \int_Y \mathbf{D}^{MI} \cdot (\mathbf{I} - \mathbf{b} \cdot \boldsymbol{\varphi}) dY \quad (11)$$

$$\mathbf{D}^{MI} = \rho^\alpha \cdot \mathbf{D}^B \quad (12)$$

Assuming \mathbf{D}^{MI} represents constitutive matrix of the material points with relative density ρ at micro-scale, \mathbf{D}^B represents the constitutive matrix of isotropic base material, where $\mathbf{I}(3 \times 3)$ is a unit matrix in two-dimensional case and $|Y|$ is the area of a unit cell, \mathbf{b} is the strain/displacement matrix. Generalized deformations of microstructure $\boldsymbol{\varphi}$ could be obtained from the two equations below,

$$\mathbf{k} \cdot \boldsymbol{\varphi} = \int_Y \mathbf{b}^T \cdot \mathbf{D}^{MI} dY \quad (13)$$

$$\mathbf{k} = \int_Y \mathbf{b}^T \cdot \mathbf{D}^{MI} \cdot \mathbf{b} dY \quad (14)$$

where deformation $\boldsymbol{\varphi}$ is a matrix which is composed of three deformation fields in two dimensional case, and Eq.

(13) is a multiple loads FEM analysis with three different loads (stiffness matrix is unchanged) for two dimensional case.

By virtue of Eqs. (6-14), we have completed the structural analysis at two scales and got the structural deformation \mathbf{U} . Then one can further obtain current objective function C based on the current design variables. The basic idea of the process above was summarized in Fig 1.

4.2 Sensitivity analysis of concurrent optimization for thermoelastic structures and materials

Sensitivity analysis is important to enhance the efficiency of the sensitivity based algorithm. Based on the equations above, it is readily to obtain the following two derivatives of objective function with respect to design variables.

$$\begin{aligned} \frac{\partial C}{\partial P_i} &= -\mathbf{U}^T \frac{\partial \mathbf{K}}{\partial P_i} \mathbf{U} + 2 \cdot \mathbf{U}^T \sum_{r=1}^N \int_{\Omega^r} \mathbf{B}^T \frac{\partial \boldsymbol{\beta}^{MA}}{\partial P_i} \Delta \mathbf{T} d\Omega^e \\ &= -\mathbf{u}_i^T \left[\left(\alpha \cdot P_i^{\alpha-1} \right) \int_{\Omega^r} \mathbf{B}^T D_i^H \mathbf{B} d\Omega^e \right] \mathbf{u}_i \\ &\quad + 2 \cdot \mathbf{u}_i^T \cdot \alpha \cdot P_i^{\alpha-1} \int_{\Omega^r} \mathbf{B}^T \boldsymbol{\beta}_i^H \Delta \mathbf{T} d\Omega^e \\ &= -\frac{\alpha}{P_i} \mathbf{u}_i^T \left[\int_{\Omega^r} \mathbf{B}^T D_i^{MA} \mathbf{B} d\Omega^e \right] \mathbf{u}_i \\ &\quad + 2 \cdot \frac{\alpha}{P_i} \mathbf{u}_i^T \int_{\Omega^r} \mathbf{B}^T \boldsymbol{\beta}_i^{MA} \Delta \mathbf{T} d\Omega^e \end{aligned} \quad (15)$$

$$\begin{aligned} \frac{\partial C}{\partial \rho_j} &= -\mathbf{U}^T \frac{\partial \mathbf{K}}{\partial \rho_j} \mathbf{U} + 2 \cdot \mathbf{U}^T \sum_{r=1}^N \int_{\Omega^r} \mathbf{B}^T \frac{\partial \boldsymbol{\beta}^{MA}}{\partial \rho_j} \Delta \mathbf{T} d\Omega^e \\ &= -\sum_{r=1}^N \mathbf{u}_r^T \left(\int_{\Omega^r} \mathbf{B}^T P_r^\alpha \frac{\partial \mathbf{D}_r^H}{\partial \rho_j} \mathbf{B} d\Omega^r \right) \mathbf{u}_r \\ &\quad + 2 \cdot \sum_{r=1}^N \mathbf{u}_r^T \left(\int_{\Omega^r} \mathbf{B}^T P_r^\alpha \frac{\partial \mathbf{D}_r^H}{\partial \rho_j} \boldsymbol{\alpha}^B \Delta \mathbf{T} d\Omega^r \right) \end{aligned} \quad (16)$$

where the derivative of \mathbf{D}^H with respect to ρ_j can be computed following references [20] as

$$\frac{\partial \mathbf{D}^H}{\partial \rho_j} = \int_Y (\mathbf{I} - \mathbf{b} \cdot \boldsymbol{\varphi})^T \cdot \frac{\partial \mathbf{D}^{MI}}{\partial \rho_j} \cdot (\mathbf{I} - \mathbf{b} \cdot \boldsymbol{\varphi}) dY \quad (17)$$

Combined with equation(12), the equation above leads to

$$\frac{\partial \mathbf{D}^H}{\partial \rho_j} = \frac{\alpha}{\rho_j} \frac{1}{|Y|} \int (\mathbf{I} - \boldsymbol{\varepsilon}_y^T(\boldsymbol{\varphi})) \mathbf{D}^{MI} (\mathbf{I} - \boldsymbol{\varepsilon}_y(\boldsymbol{\varphi})) dY \quad (18)$$

The derivatives of Constraint I with respect to design variables can be written as,

For the perimeter control only is applied on the micro-scale, then

$$\frac{\partial \zeta}{\partial P_i} = \frac{\rho^{PAM} A_i^{MA}}{V^{MA} \zeta}; \quad \frac{\partial \zeta}{\partial \rho_j} = \frac{a_j^{MI} \cdot \int_{\Omega} P d\Omega}{V^{MA} \cdot V^{MI} \cdot \zeta} \quad (19)$$

The derivatives of Constraint II with respect to design variables can be written as,

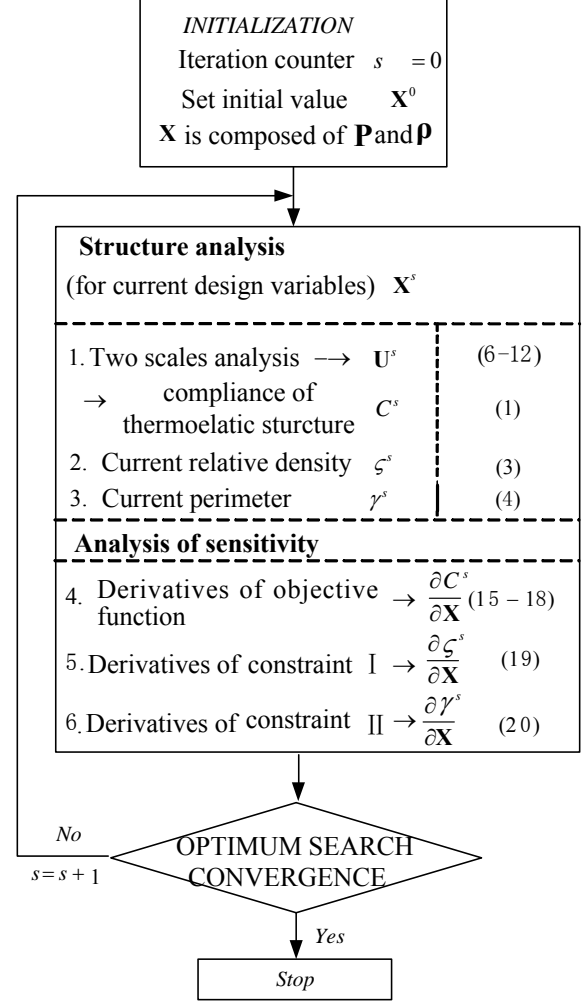


Fig. 2. Flow chart of concurrent optimization for thermoelastic structure and material

$$\frac{\partial \gamma}{\partial P_i} = 0; \quad \frac{\partial \gamma}{\partial \rho_j} = \frac{2 \cdot \sum_{j=1}^m l_j (\rho_{j1} - \rho_{j2})}{\gamma} \quad (20)$$

A^{MA} , α^{MI} , V^{MA} and V^{MI} represents the area of elements and design domain at macro- and micro- scales. Now, we have completed the structural analysis and sensitivity analysis. A flow chart of key steps and corresponding equations is given in Fig 2.

Table 1. The influence of temperature differential on the concurrent design results

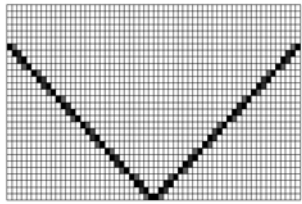

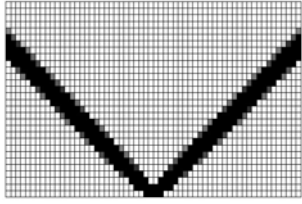
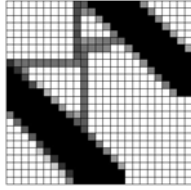
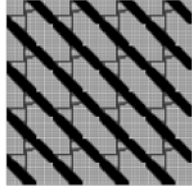
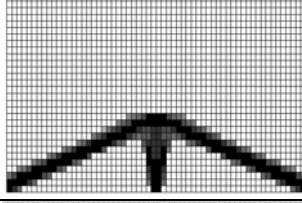
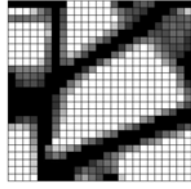
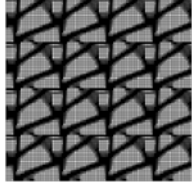
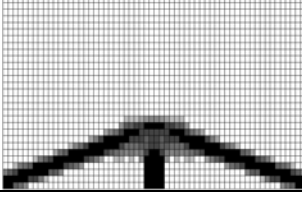
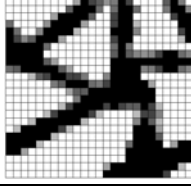
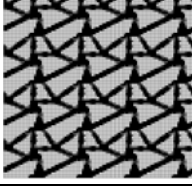
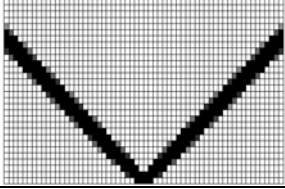
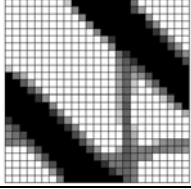
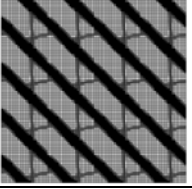
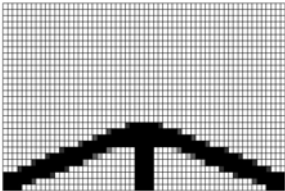
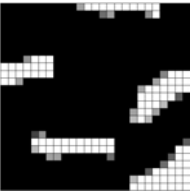
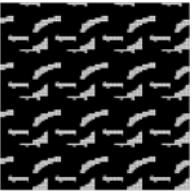
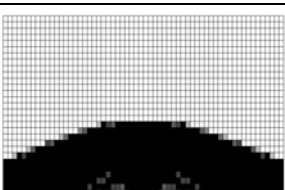
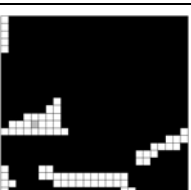

T	Structural topology	Microstructural topology	
		Unit Cell	3×3 arrays
0° C			
4° C			
20° C			
40° C			

Table 2 Influence of base material volume on the concurrent optimization design

V	P^{SIM}	ρ^{PAM}	Compliance	Structural topology	Microstructural topology	
					Unit Cell	3×3 arrays
5%	0.1326	0.3772	47770			
20%	0.2191	0.9126	17664			
30%	0.3409	0.8742	14597			

5 Numerical Examples

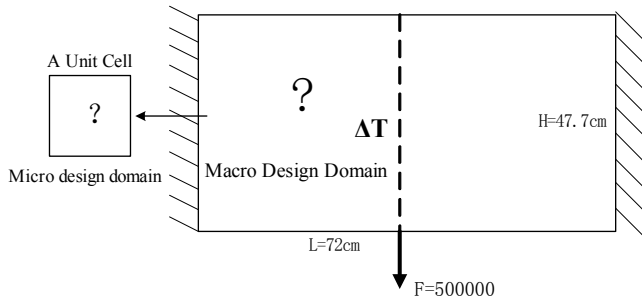


Fig. 3. Numerical example

The initial design domain is shown in Fig 3. The dimensions are $72\text{cm} \times 47.7\text{cm} \times 1\text{cm}$, the applied load has a value of $F=500000\text{N}$, the right and left sides of the structure are clamped and the whole design domain has a temperature differential of ΔT . Base material is assumed to have Young's modulus $E^B = 100\text{GPa}$, Poisson's ratio $\nu^B = 0.3$ and thermal expansion coefficient of $\alpha^B = \{1.0 \times 10^{-5}, 1.0 \times 10^{-5}, 0\}^T$. Due to the symmetry of the problem, only the left half part is considered as macro design domain (the configuration of micro-structure in right part can be obtained as mirror of counterpart of left part). The mesh is 60×30 for macro design domain and 25×25 for the microstructure (8-Node Planar Element). OPTIMUM SEARCH is implemented by the optimization package DOT using the SQP (Sequential Quadratic Programming) algorithm [21].

The influence of temperature differential on the concurrent design results are discussed in Table 1. Here upper bound of perimeter constraint is set to be $\bar{\gamma}$, and the volume constraint is equal to 5% of the total volume.

The first row of the Table 1 shows the case of no effects due to thermal loads, i.e. $\Delta T=0$, case in which the concurrent optimization for thermoelastic structures degenerates to optimization for elastic structure with mechanical loads alone. In this case, it is interesting to note that the “two-bar like” configuration appears for the macro-structure and there is no cellular structure in the result configuration of microstructures, equivalently the optimum microstructure is isotropic solid material ($\rho_{Opt}^{PAM} = 1$). Is the use of porous material not good for improving stiffness of the structures with mechanical loads only? More numerical examples indicate it is true except for the structures in a uniaxial stress case as far as the authors know. The reason for this, we believe, is the assumption of uniform configuration of micro-structure. States of stress in the structures are usually complex and the directions of principle stress at different material points could be arbitrary and the best design for material configuration is to distribute the base material along the directions of principle stress at certain material point. Thus to meet the different requirements of material distribution at different points in structures with uniform micro-structure configuration, the isotropic solid material might be the best choice. On the other hand, the microstructural configuration of porous material actually imposes a kind of constraint on the distribution of base material in whole structure system with an assumed uniform micro-structure configuration. Compared

with the constrained distribution when porous material is used, the base material can be distributed more freely when the isotropic solid material is used to obtain better system performance. More explanations could be done from the point view of sensitivity analysis, which might be done in the near future study.

When $\Delta T \neq 0$, the thermal loads, together with the mechanical loads, have effects on the optimization results, and in this case we found the cellular material could help to reduce the compliance of system from the observations of the results in the 2nd to 5th rows of Table 1. As we can see in rows 2-5, when the temperature differential is small, the mechanical loads governing, the configuration of macro-structure shows a “two-bar” configuration. With increasing of temperature differential, it tends to transform to “three-bar” configuration that reflects greater effect of thermal loads. For “three-bar” configuration, central force could be balanced partly by the sum force from the two oblique bars due to temperature improvement. Then the displacements, also the system compliance, could be reduced by this configuration. When the mechanical loads dominate, the base material is distributed along the direction of axis of “macro-bar” at micro-scale; when no load dominate, a complex configuration appears which reflects combined effects of mechanical and thermal loads.

Table 2 shows optimization results with varying volume fraction of base material $\bar{\zeta}$, where the upper bound of perimeter constraint is set to be a proper value $\bar{\gamma} = 2$ based on experience obtained from numerical simulation, and the temperature differential is set to be $\Delta T = 2^\circ\text{C}$.

$$P^{SIM} = \frac{\int_{\Omega} P_i d\Omega}{V^{MA}}$$
 and ρ^{PAM} represent the distribution volume fractions of base material at macro and micro scales.

As shown in the table above, relative density of micro unit cell ρ^{PAM} and macro scale P^{SIM} both increase as volume fraction of base material increase from 5% to 20%, but the increasing rate of relative density of micro unit cell far exceeds its counterpart. At the same time, the configuration of macro-structure transforms from the “two-bar” to the “three-bar” and there is a corresponding reduction in system compliance. But when the volume fraction of base material increase further from 20% to 30%, the relative density of micro unit cell does not approach $\rho^{PAM} = 1$ as expected, but begins to reduce. The volume fraction of macro-structure tends to increase substantially and the system compliance can reduce further when the configuration of macro-structure tends to be a horizontal bar.

And Figs. 4 and 5 give the trends of actually used material volume fraction and macro/micro volume fraction with increasing of specified material volume fraction. In figure 4, we can see a linear increase of actually used material volume fraction with that of specifying when the specified volume fraction is less than 35%. After that, an obvious plateau in the figure can be observed, which is corresponding to the optimum material volume fraction mentioned above. The macro/micro volume fractions and configuration remain stable after the optimum volume fraction. And the volume constraint, constraint II, is no longer an active one after the optimum volume fraction also.

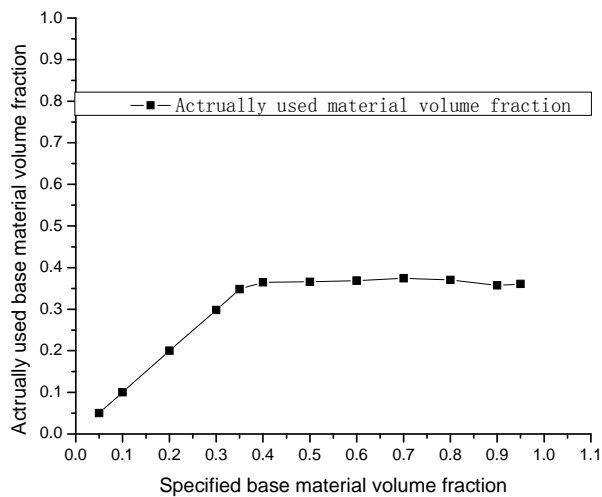


Fig. 4. Trend of actually used material volume with increasing of specified material volume fraction

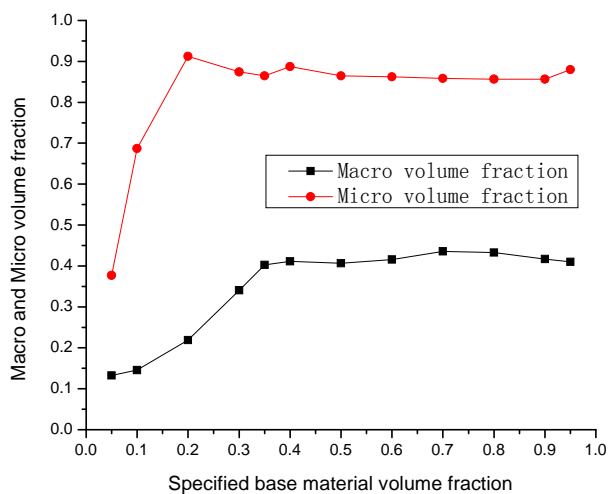


Fig. 5. Trend of macro/micro volume fraction with increasing of specified material volume fraction

6 Conclusion remarks

A new strategy of concurrent optimization design of macro-structure and micro-structure for the thermoelastic structures under combined mechanical and thermal loads is proposed. By this method, the optimum material microstructure configuration according to different macro structure configurations, loads and constraints could be obtained for thermoelastic structures. Macro and micro densities are chosen as the design variables for structure and material microstructure independently and integrated into one system with the help of homogenization theory and the penalization approaches (SIMP at micro-scale and PAMP at macro-scale) to ensure clear topologies. The distribution of base material between the structure and material can be decided automatically by the optimization model. At the same time, microstructure is assumed to be uniform in macro-scale to reduce manufactur-

ing cost. Numerical results in this paper proved the viability of the method and model. With this strategy it is found that for the cases in which only mechanical loads apply, micro-structure of isotropic solid material is best for achieving the minimum structural compliance; while for the cases in which both mechanical and thermal loads apply, the configuration of porous material is more effective to reduce the system compliance. So it will be an interesting and challenging work to extend this concurrent optimization method to multifunctional applications, e.g. integrate heat transfer, vibration isolation and mechanical requirements into one system.

Acknowledgements

The financial support for this research was provided by National Basic Research Program of China through Grant No. 2006CB601205 and the Major Program (10332010) and the Innovative Research Team Program (10421002) of NSFC and the start funds for research of DUT. These supports are gratefully appreciated.

References

1. G.D. Cheng. *On Non-Smoothness in Optimal Design of Solid Elastic Plates*. International Journal of Solids and Structures, **17**, 795-810 (1981).
2. B. Hassani, E. Hinton. *A review of homogenization and topology optimization III - topology optimization using optimality criteria*. Computers and Structures, **69**, 739-756 (1998).
3. M.P. Bendsoe, O. Sigmund. *Topology Optimization: Theory Methods and Applications*. (Berlin: Springer-Verlag, 2003).
4. H. Rodrigues, P. Fernandes. *A material based model for topology optimization of thermoelastic structures*. International Journal for numerical methods in engineering, **38**, 1951-1965 (1995).
5. B. Wang. *Design of cellular structures for optimum efficiency of heat dissipation*. Structural and Multidisciplinary Optimization, **30**, 447-458 (2005).
6. M.P. Bendsoe, O. Sigmund. *Material interpolation schemes in topology optimization*. Archive Of Applied Mechanics, **69**, 635-654 (1999).
7. R.B. Haber, C.S. Jog, M.P. Bendsoe. *A new approach to variable-topology shape design using a constraint on perimeter*. Structural Optimization, **11**, 1-12 (1996).
8. O. Sigmund. *Design of material structures using topology optimization*, PhD thesis, (Department of Solid Mechanics, Technical University of Denmark, 1994).
9. O. Sigmund, J. Petersson. *Numerical instabilities in topology optimization: A survey on procedures dealing with checkerboards, mesh-dependencies and local minima*. Structural Optimization, **16**, 68-75 (1996).
10. H. Rodrigues, J.M. Guedes, M.P. Bendsoe. *Hierarchical optimization of material and structure*. Structural And Multidisciplinary Optimization, **24**, 1-10, (2002).
11. L. J. Gibson, M. F. Ashby. *Cellular Solids: Structure and Properties*. (Cambridge: Cambridge University Press, 1997.)
12. e. a. A.M. Hayes. *Mechanics of linear cellular alloys*. Mechanics of Materials, **36**, 691-713, (2004).
13. N. Wicks, J.W. Hutchinson. *Optimal truss plates*. International Journal of Solids and Structures, **38**, 5165-5183,

- (2001).
14. S. Hyun, S. Torquato. *Optimal and manufacturable two-dimensional, Kagome-like cellular solids*. Journal Of Materials Research, **17**, 137-144, (2002).
 15. S. Gu, T.J. Lu, A.G. Evans. *On the design of two-dimensional cellular metals for combined heat dissipation and structural load capacity*. International Journal of Heat and Mass Transfer, **44**, 2163-2175, (2001).
 16. O. Sigmund. *Tailoring materials with prescribed elastic properties*. Mechanics of Materials, **20**, 351-368, (1995).
 17. J. Yan, L. Ling, G. Cheng, *Comparison of and Scale effects on prediction of equivalent elastic property and the shape optimization of truss material with periodic microstructure*. Internatioanl Journal of Mechanical Science, **48**, 400-413, (2006).
 18. W.H. Zhang, P. Duysinx. *Dual approach using a variant perimeter constraint and efficient sub-iteration scheme for topology optimization*. Computers & Structures, **81**, 2173-2181, (2003).
 19. S. Liu, G. Cheng. *Homogenization-based method for predicting thermal expansion coefficients of composite materials*. Journal of Dalian University of Technology, **35**, 451-457, (1995).
 20. S. Liu, G. Cheng, Y. Gu. *Mapping method for sensitivity analysis of composite material property*. Structural And Multidisciplinary Optimization, **24**, 212-217, (2002).
 21. G. N. Vanderplaats. *Design optimization tools user's manual*, (Vanderplaats Research & Development Inc., Colorado, 1999).